Published in final edited form as:

Photochem Photobiol. 2017 July ; 93(4): 1016–1024. doi:10.1111/php.12758.

Naproxen Inhibits UVB-induced Basal Cell and Squamous Cell Carcinoma Development in Ptch1$^{+/-}$/SKH-1 hairless mice

Sandeep C. Chaudhary[1,*], **Mohammad Waseem**[1], **Mehtab Rana**[1], **Hui Xu**[1], **Levy Kopelovich**[2], **Craig A. Elmets**[1], and **Mohammad Athar**[1,*]

[1]Department of Dermatology, VH509 University of Alabama at Birmingham, Birmingham, AL 35294-0019, USA

[2]Department of Medicine, Weill Cornell Medical College, New York, NY 10065, USA

Abstract

Naproxen possesses anti-proliferative and pro-apoptotic effects besides its known anti-inflammatory functions. Here, we demonstrate the anti-cancer effects of naproxen against UVB-induced BCCs and SCCs in a highly susceptible murine model of UVB carcinogenesis. Naproxen significantly inhibited UVB-induced BCCs and SCCs in this model. Tumor number and volume were significantly decreased ($p<0.005$ and $p<0.05$, respectively). Inhibition in UVB-induced SCCs and BCCs was 77% and 86%, respectively, which was associated with reduced PCNA and cyclin D1 and increased apoptosis. As expected, inflammation-related iNOS, COX-2, and nuclear NFκBp65 were also diminished by naproxen treatment. Residual tumors excised from naproxen-treated animal were less invasive and showed reduced expression of epithelial-mesenchymal transition (EMT) markers N-cadherin, Vimentin, Snail, and Twist with increased expression of E-cadherin. In BCC and SCC cells, naproxen induced apoptosis and activated unfolded protein response (UPR) signaling with increased expression of ATF4, p-eIF2α, and CHOP. Employing iRNA-based approaches, we found that naproxen-induced apoptosis was regulated by CHOP as sensitivity of these cutaneous neoplastic cells for apoptosis was significantly diminished by ablating CHOP. In summary, these data show that naproxen is a potent inhibitor of UVB-induced skin carcinogenesis. ER stress pathway protein CHOP may play an important role in inducing apoptosis in cancer cells.

Keywords

Naproxen; photocarcinogenesis; skin; UVB; inflammation; UPR signaling

Introduction

Non-melanoma skin cancers (NMSCs) including basal cell carcinoma (BCC) and squamous cell carcinoma (SCC), are the most commonly diagnosed cancers in the US. It was reported that the incidence of these skin cancers is higher than the total incidence of various other

*Address for Correspondence: Sandeep C. Chaudhary, Ph.D. (scc09@uab.edu) and Mohammad Athar, Ph.D. (mathar@uabmc.edu), Department of Dermatology, University of Alabama at Birmingham, 1530 3rd Avenue South, VH 509, Birmingham, AL 35294-0019, USA. Phone: 205-934-7554, Fax: 205-934-7500.

cancers such as breast, prostate, lung, and colon (1). Solar ultraviolet B (UVB) radiation (280–320 nm) is the major etiologic factor. Artificial tanning is also known to enhance the risk for the skin cancer development (2). Solar UVB is a complete carcinogen. UVB-mediated DNA damage, inflammatory and suppressed immune responses and altered multiple cell signaling pathways together are considered to be involved in the development of epidermal neoplasm (3). NMSCs can be excised and cured if diagnosed early. Additionally, prevention could be the best strategy to diminish the incidence of these cancers (4). Our laboratory has focused on identifying on various pharmacological targets for the intervention of UVB-induced NMSCs in various murine models. Accordingly, effects of inhibition of pathways such as cyclooxygenase (COX), ornithine decarboxylase, p53, sonic hedgehog, estrogen receptor and Wnt have been described earlier (5–12).

The NSAIDs (non-steroidal anti-inflammatory drugs) include both selective and nonselective COX2 inhibitors. Many of these drugs have been evaluated in our and other laboratories for their anticancer efficacy. Some of these agents also showed high efficacy in *in vitro* and in preclinical models (13, 10, 11, 14). However, use of these NSAIDs is not free from other toxic side effects in humans (15). For example, specific COX-2 inhibitors have been associated with high risk of cardiovascular toxicity in humans. Nonetheless, later it was shown that these NSAIDs-associated cardiac events more frequently occur in high risk populations (16). Among NSAIDs, naproxen is an over-the-counter medicine and has been widely used. Its anti-proliferative, pro-apoptosis, and anti-inflammatory effects have also been demonstrated both in experimental models of various tumor-types and in human cancer cells (17, 18). Initially, molecular basis for the efficacy of NSAIDs was shown to be mainly due to inhibition of the enzyme activity of cyclooxygenases (COXs). Therefore, it was thought that these agents by reducing prostaglandins (PGs) production particularly PGE_2 levels in cancer cell as well as in the tumor microenvironment affect multiple signaling pathways involved in cancer progression (19–21). Recently, in a computer based-kinase screening from the Protein Data Bank ligand database and pull-down assay, it was shown that naproxen blocks kinase activity of phosphoinositide 3-kinase (PI3K) by directly binding with PI3K and inducing apoptosis in N-butyl-N-(4-hydroxybutyl)-nitrosamine-induced rat urinary bladder cancer (22). Recent interest in these agents has also grown due to the demonstration that evasion of tumor immunity involves COXs as a significantly important mechanism of tumor growth promotion (23). These recent findings suggest the multifarious roles of NSAIDs including naproxen.

In present study, we investigated cancer chemopreventive and cancer cell proliferation inhibiting effects of naproxen on the UVB-induced SCCs and BCCs. Using a unique mouse model, $Ptch1^{+/-}$/SKH-1 hairless which is highly sensitive to UVB, we show that naproxen reduces tumors developed by chronic UVB irradiation of these animals. We observed a potent cancer chemopreventive activity of naproxen against both SCCs and BCCs. These tumor inhibitory effects of naproxen were accompanied by a significant reduction in pro-inflammatory responses and epithelial-mesenchymal transition (EMT). We also showed that CHOP-mediated apoptosis in SCC and BCC cells by naproxen, could be the underlying molecular mechanism.

Materials and Methods

Reagents and Animals

Naproxen ($C_{14}H_{14}O_3$) was procured from Focal Vision International Pvt. Ltd., Mumbai, India and stored at room temperature. Six- to eight-weeks-old Ptch1$^{+/-}$/SKH-1 hairless female mice were used for this study. Ptch1$^{+/-}$/SKH-1 hairless mice were generated and genotyped as described earlier (12). The animals were housed under standard conditions of constant temperature of 24 ± 2°C and relative humidity of 50 ± 10%, and were maintained on a 12 h light/12 h dark cycle with food and drinking water *ad libitum*. The animal studies were conducted under an approved protocol by the Institutional Animal Care and Use Committee (IACUC) of the University of Alabama at Birmingham.

UV light source

The UV irradiation unit (Daavlin Co., Bryan, OH) was used in the study. The irradiation unit was equipped with six Philips Ultravoilet B TL 40W/12RS lamps and with an electronic controller to regulate dose. We also used a Kodacel cellulose film (Kodacel TA401/407) to eliminate UVC as described earlier (10).

Experimental Protocol

To study the efficacy of naproxen on UVB-induced skin carcinogenesis, the animals were randomly divided into three groups. The animals of group I which received no treatment served as age-matched vehicle controls (negative control). Group II and group III animals were irradiated with UVB (180 mJ/cm^2; twice/week) for 30 weeks. In addition, group II and group III animals received parenteral administration of PBS or naproxen (1 mg/mouse in 100 µl PBS, i.p.), respectively. The tumor number and size of each tumor bearing mouse were measured weekly using electronic Vernier Caliper. Tumor volume was calculated using formula: tumor volume = length × width × height as described earlier (12). Data were presented as mean±SE and plotted as a function of weeks on test. After UVB irradiation for 30 weeks, the experiment was terminated and all mice were euthanized as approved by our IACUC protocol. The harvested skin and tumor tissues were processed for histological and biochemical analysis as described below.

Histology, Immunohistochemistry, Immunofluorescence staining and Terminal deoxynucleotidyl transferase–mediated nick end labeling (TUNEL) assay

Tissues specified for histological evaluation were fixed in 10 % neutral-buffered formalin, embedded in paraffin, and cut in serial 5 µm. Paraffin sections were used for the histologic determination of skin and tumors. For skin/tumor histological evaluation, the tissue sections were stained with H&E and examined for skin or tumor histology. Vector Red Alkaline Phosphatase Substrate Kit (Cat no. SK5100) was used for immunohistochemistry as per manufacturer's guidelines. For immunofluorescence staining, deparaffinized and rehydrated sections following epitope retrieval using antigen unmasking solution (Vector laboratories) for 20 min at 95°C and blocking nonspecific sites with 2 % BSA for 45 min at room temperature, were incubated with specific primary antibody overnight at 4°C. The sections were then washed with PBS (1X) and probed with secondary antibody coupled using Alexa

Fluor 594 (Invitrogen, Carlsbad, CA, USA) or Fluorescein (Pierce)-coupled secondary antibody. Finally, sections were washed and mounted with Vectashield Mounting Medium with DAPI (H-1200; Vector Laboratories). *In situ* cell death detection kit (Roche Applied Science) was used for TUNEL assay as per manufacturer's guidelines.

Cell culture and treatment

Human epidermoid carcinoma (A431) cells were purchased from the American Type Culture Corporation (Manassas, VA, USA). A431 cells were grown in DMEM containing 10 % fetal bovine serum (FBS), 100 U/ml of penicillin, and 100 μg/ml of streptomycin. Murine-derived basal cell carcinoma (ASZ001) cells were maintained in 154CF medium as reported previously (24). All cell lines were routinely cultured in the recommended growth medium and maintained in humidified incubators at 37°C under 5% CO_2. Cells (60–70% confluent) were treated with naproxen or vehicle (PBS) in complete culture medium. After 24 h of treatment, medium was removed and the cells were harvested and whole-cell lysates prepared. For siRNA-mediated CHOP-silencing, A431 and ASZ001 cells were seeded in a 24-well plate and transfected with CHOP siRNA (10 nM). After 24 h, cells were fixed and TUNEL staining was performed on fixed cells according to manufacturer's guideline.

Western blot analysis

Western blot analysis was performed with total cell or tissue lysates which were prepared using ice-cold lysis buffer as described earlier (12). Briefly, 40–80 μg proteins were separated on 10–15% SDS-PAGE and transferred onto a nitrocellulose membrane (BioRad, CA, USA). After blocking with 5% non-fat dry milk, the membrane was incubated with specific primary antibody (PCNA, Santa Cruz; Cyclin D1, Neomarker; Bax, Cell Signaling; Bcl2, Cell Signaling; p-NFκBp65, Abcam; COX-2, Abcam; iNOS, Abcam; Snail, Abcam; E-cadherin, Santa Cruz; Vimentin, Abcam; Twist, Abcam; N-cadherin; Santa Cruz; Cleaved caspase3, Cell Signaling; CHOP, Cell Signaling; p-eIF2α, Cell Signaling; eIF2α, Cell Signaling; ATF4, Cell Signaling; GRP78, Cell Signaling and β-actin, Sigma) overnight at 4°C. The membrane was washed and probed with appropriate HRP-conjugated secondary antibodies (1:2,000 dilutions). Finally, the membrane was washed and developed using the enhanced chemiluminescence reagent (Pierce, Rockford, IL, USA). One membrane was stripped multiple times to probe with new antibodies. In some cases where proteins which were probed had significant molecular weight differences, the membrane was cut into two halves and probed. Membranes were stripped and re-probed with β-actin. Therefore, same β-actin represented as loading control for multiple proteins. Density of Western blots was analyzed by using IMAGE J software (http://rsbweb.nih.gov/ij/).

Colony forming assay

Colony forming ability of A431 and ASZ001 cells was measured with or without naproxen. Briefly, the cells were trypsinized, washed and seeded into 6-well plates (500 cells/well). These cells were then allowed to grow overnight and treated with vehicle or naproxen. These cells were incubated in humidified chamber at 37°C for additional 10 days. Cell colonies were fixed with 4% paraformaldehyde for 5 minutes and stained with 0.5% crystal violet for 30s. Finally, cell colonies were examined and their numbers were counted.

Densitometry and statistical analysis

All values are expressed as mean ± SE. Microsoft Excel software 2007 was used to perform statistical analysis. Student's *t-test* was used to test the significance between two test groups. A 'p'-value of <0.05 was considered to be significant.

Results

Naproxen inhibits UVB-induced SCC and BCC development in Ptch1$^{+/-}$/SKH-1 hairless mice

Administration of naproxen substantially reduced the progression of UVB-induced skin tumors in Ptch1$^{+/-}$/SKH-1 hairless mice as compared to vehicle-treated and UVB (alone)-irradiated mice. At week 30th, a significant reduction in tumor number ($p<0.005$) and tumor volume ($p<0.05$) was observed in naproxen-treated mice (Fig. 1a and b). However, the tumor incidence in the two groups was not significantly different. The percentage of mice bearing tumors in naproxen-treated group was 80% of UVB-irradiated group (data not shown). The average number of tumors was decreased to 2.9±0.75/mouse in naproxen group from 10.2±2.45/mouse in UVB (alone) group, which corresponded to more than 70% reduction in tumor numbers (Fig. 1a). A significant reduction (~63%; $p<0.05$) in tumor/tumor-bearing mouse was also noted in naproxen-treated group (data not shown). Similarly, the average tumor volume was also considerably decreased (59%; $p<0.05$) in mice treated with naproxen (Fig. 1b). Ptch1$^{+/-}$/SKH-1 mouse is a highly susceptible murine model as it develops both SCC and BCC following chronic irradiation of UVB as described earlier (12). To assess the effects of naproxen administration on the development of UVB-induced SCC, BCC, and papilloma in these mice, we performed tumor distribution analysis in naproxen-treated and untreated groups. Tumor distribution in UVB-irradiated Ptch1$^{+/-}$/SKH-1 mice was 22% SCC, 22% BCC, and 56% papilloma. Naproxen treatment significantly reduced UVB-induced SCC (86%, $p<0.05$), BCC (77%, $p<0.05$), and papilloma (62%, $p<0.05$) (Fig. 1c, d and e). Analysis of microscopic BCC showed that UVB irradiation significantly enhanced BCC development (2.75±0.88 microscopic BCC/unit area mm^2 of skin; $p<0.05$) as compared to spontaneous BCC growth in age-matched control (0.17±0.08 microscopic BCC/unit area mm^2). Please note that a few of the age-matched control Ptch1$^{+/-}$/SKH-1 mice also develop some spontaneous BCCs as shown in the control section (Fig. 1f and g). Naproxen treatment significantly reduced BCC growth (0.73±0.39 microscopic BCC/unit area mm^2) (Fig. 1f and g).

Thus, it seems likely that administration of naproxen reduced the progression of papilloma to SCC and microscopic BCC to visible BCC in Ptch1$^{+/-}$/SKH-1 mice. Furthermore, histological analysis showed that UVB induced poorly differentiated SCC as characterized by the presence of spindle cells with pleomorphic nuclei, lack of keratin pearls, high mitotic activity, and invasive growth progression in the dermis. Interestingly in naproxen treatment group, most of the SCCs were highly differentiated characterized by presence of small well-developed keratin pearls, and infrequent dermal invasion (Fig. 2a).

Naproxen reduces proliferation and induces apoptosis in UVB-induced SCC and BCC

We next investigated the expression pattern of proliferation biomarkers PCNA and Cyclin D1 in SCC, BCC and skin-adjacent tissues by immunostaining and Western blot analysis. Analysis of UVB-induced SCC, BCC as well as tumor-adjacent tissue reveals that a large number of epidermal cells were positive for PCNA and Cyclin D1 staining (Fig. 2b, c and d). Naproxen treatment significantly ($p<0.05$) reduced the expression of these proliferation biomarkers in both SCC and BCC and as well as in tumor-adjacent tissues (Fig. 2b, c and d). As shown in fig. 2e, compared to their respective UVB-irradiated SCC and BCC, the number of TUNEL-positive cells in tumor lesions was significantly enhanced by naproxen treatment. Of note, we also observed significant increase in TUNEL-positive cells in tumor-adjacent skin of naproxen-treated animals (data not shown). Additionally, the expression of pro-apoptotic protein Bax and anti-apoptotic Bcl2 in tumor-adjacent skin was also altered to favor the induction of apoptosis in the skin and tumors excised from naproxen-treated animals (Fig. 2f).

Naproxen treatment reduces pro-inflammatory signaling and dampens epithelial-mesenchymal transition (EMT) process in UVB-induced SCC and BCC

UVB irradiation is known to induce cutaneous and systemic inflammation signaling responses (25, 26). This inflammatory response is accompanied by the cytokine production, induction of prostaglandin synthesis, activation of nuclear factor kappa B and its dependent signaling in the epidermal keratinocyte and skin-associated other cells (25–28). Transcriptionally active NFκBp65 plays central role in inducing expression of proinflammatory mediators (29, 30). Earlier, it has been demonstrated IκB kinase (IKK)–mediated phosphorylation of IκB induces the activation of NFκB transcription which induces transcription of its target genes. In immunofluorescence staining, we observed that phosphorylated NFκBp65 localized to the nucleus of UVB-induced SCCs was drastically reduced by naproxen treatment (Fig. 3a). Concomitantly, expression of its target proteins COX2 and iNOS was also diminished (Fig. 3b). Pro-inflammatory tumor microenvironment is often known to facilitate the progression of invasive lesions (31, 32). A downregulation of E-cadherin, N-cadherin, vimentin, fibronectin in addition to EMT regulating transcription factors SNAI and twist were noted in UVB-induced lesions which is consistent with earlier observation (33, 34). As observed in immunofluorescence staining, the expression of Snail, Twist, Vimentin, and N-cadherin was decreased in tumor tissues harvested from naproxen-treated mice with concomitant increase in E-cadherin in these tissues (Fig. 3c and d).

Naproxen activates unfolded protein response (UPR) and induces CHOP-mediated apoptosis in SCC and BCC cells *in vitro*

To unravel the molecular mechanism of action of naproxen, we employed the human epidermoid carcinoma A431 cells and murine basal cell carcinoma-derived ASZ001 cells. These cells were treated with various concentrations of naproxen (0–10 mM) for cell growth assay. Cells treated with naproxen for 24 h decreased the cell growth in dose-dependent manner (Fig. 4a and b). Similarly naproxen treatment significantly ($p<0.001$) reduced the colony forming potential of these cells (Fig. 4c and d). In Western blot analysis, we observed that naproxen treatment of A431 and ASZ0001 cells decreased the expression of anti-

apoptotic protein Bcl2 and increased cleaved caspase 3 (Fig. 4e). One possible trigger for apoptosis induction may be via unfolded protein response (UPR) signaling-regulated protein CHOP (C/EBP-homologous protein) (35, 36). Early studies demonstrated that CHOP interacts with various transcription factors and decrease the expression of pro-survival protein Bcl2 leading to apoptosis (37, 38). We noted an increased expression of CHOP in naproxen-treated A431 and ASZ001 cells with the concomitant increase in other UPR signaling proteins such as phosphorylated eIF2α (eukaryotic initiation factor 2α), ATF4 (activating transcription factor 4), and GRP78 (Glucose-Regulated Protein 78) (Fig. 4e). To confirm the role of CHOP in naproxen-induced apoptosis cell, we employed small interference RNA-based approach to knockdown CHOP in A431 and ASZ001 cells. Then these cells were treated with naproxen. Blockade of CHOP significantly decreased the number of TUNEL-positive apoptotic cells following naproxen treatment (Fig. 4f and g).

Discussion

A number of epidemiological and experimental studies suggest that COX-2 is overexpressed in a large number of human malignancies including skin cancer (5, 13, 14, 23). We have shown that increased COX-2 plays important roles in the pathogenesis of both BCC and SCCs (5, 39, 40). While COX-2-mediated production of PGE_2 plays key roles in tumor progression and metastasis via binding to its receptors EP1–4, these responses are distinct in BCCs vs SCCs (41, 42). In addition, we and others have shown that tumor proliferation and reduction in apoptosis by UVB-induced COX-2 involve activation of a number of signaling pathways including Akt (6, 14). Thus, administration of both specific and non-specific inhibitors of COX-2 provides benefit in intercepting tumor growth (43). However, underlying mechanisms mediating these effects are not clearly understood. Recent elegant studies have suggested that COX-2 is involved in augmenting tumor growth via envasion of immunity (23). In this regard, it has been shown that COX in tumor cells induces PGE_2 that subverts the myeloid cell function. Moreover, COX expression ablation in tumors enabled immune control, while COX-2 inhibition synergized with checkpoint blockade therapy (23). Our observations though very preliminary, point to a novel mechanism by which naproxen may induced apoptosis in UVB-induced BCCs and SCCs. The observed induction of UPR signaling regulated transcription factor ATF4-dependent responses including augmented phosphorylation of translation initiation factor eIF2α and apoptosis regulatory protein CHOP may be the underlying mechanisms by which naproxen exerts its anti-tumor effect. While eIF2α may lead to global translation block, CHOP may augment apoptosis in tumor cells. It is intriguing in this regard that a novel mechanism by which NSAIDs act has also recently been described. It involves COX activity-independent inhibition of caspase activity and –dependent regulation of anti-inflammatory effects of NSAIDs including of naproxen (44). Therefore, it is difficult to predict how these contradictory effects are regulated in cancer cells leading to blockade of neoplastic growth. In summary, our studies describe the cancer chemoprevention activity of naproxen against both UVB-induced BCCs and SCCs in a relevant murine model. The underlying molecular mechanism may involve activation of proliferation inhibitory and apoptotic inducing responses by ATF4-dependent pathway including enhancement in hyperphosphorylated eIF2α and CHOP expression as depicted in

the flow diagram in Fig. 5. Additional studies are required to further clarify the mechanistic cascade regulating these events.

Acknowledgments

This work has been supported in part by R01CA138998 and R01ES026219 to MA and R01CA193885 to CAE.

References

1. Cancer Facts and Figures. American Cancer Society; 2016. http://www.cancer.org/acs/groups/content/@research/documents/document/acspc-047079.pdf [Accessed March 17, 2016]
2. El Ghissassi, Baan FR, Straif K, Grosse Y, Secretan B, Bouvard V, Benbrahim-Tallaa L, Guha N, Freeman C, Galichet L, Cogliano V. Special report: policy. A review of human carcinogens--part D: radiation. Lancet Oncol. 2009; 10:751–2. [PubMed: 19655431]
3. Bickers DR, Athar M. Oxidative stress in the pathogenesis of skin disease. J Invest Dermatol. 2006; 126:2565–2575. [PubMed: 17108903]
4. Umar A, Dunn BK, Greenwald P. Future directions in cancer prevention. Nat Rev Cancer. 2012; 12:835–848. [PubMed: 23151603]
5. Elmets CA, Ledet JJ, Athar M. Cyclooxygenases: mediators of UV-induced skin cancer and potential targets for prevention. J Invest Dermatol. 2014; 134:2497–2502. [PubMed: 24804836]
6. Arumugam A, Weng Z, Talwelkar SS, Chaudhary SC, Kopelovich L, Elmets CA, Afaq F, Athar M. Inhibiting cycloxygenase and ornithine decarboxylase by diclofenac and alpha-difluoromethylornithine blocks cutaneous SCCs by targeting Akt-ERK axis. PloS one. 2013; 8:e80076. [PubMed: 24260338]
7. Xu J, Timares L, Heilpern C, Weng Z, Li C, Xu H, Pressey JG, Elmets CA, Kopelovich L, Athar M. Targeting wild-type and mutant p53 with small molecule CP-31398 blocks the growth of rhabdomyosarcoma by inducing reactive oxygen species-dependent apoptosis. Cancer Res. 2010; 70:6566–6576. [PubMed: 20682800]
8. Tang X, Zhu Y, Han L, Kim AL, Kopelovich L, Bickers DR, Athar M. CP-31398 restores mutant p53 tumor suppressor function and inhibits UVB-induced skin carcinogenesis in mice. J Clin Invest. 2007; 117:3753–3764. [PubMed: 18060030]
9. Chaudhary SC, Singh T, Talwelkar SS, Srivastava RK, Arumugam A, Weng Z, Elmets CA, Afaq F, Kopelovich L, Athar M. Erb-041, an estrogen receptor-beta agonist, inhibits skin photocarcinogenesis in SKH-1 hairless mice by downregulating the WNT signaling pathway. Cancer Prev Res (Phila). 2014; 7:186–198. [PubMed: 24217507]
10. Chaudhary SC, Singh T, Kapur P, Weng Z, Arumugam A, Elmets CA, Kopelovich L, Athar M. Nitric oxide-releasing sulindac is a novel skin cancer chemopreventive agent for UVB-induced photocarcinogenesis. Toxicol Appl Pharmacol. 2013; 268:249–255. [PubMed: 23274568]
11. Singh T, Chaudhary SC, Kapur P, Weng Z, Elmets CA, Kopelovich L, Athar M. Nitric Oxide Donor Exisulind Is an Effective Inhibitor of Murine Photocarcinogenesis(dagger). Photochem Photobiol. 2012
12. Chaudhary SC, Tang X, Arumugam A, Li C, Srivastava RK, Weng Z, Xu J, Zhang X, Kim AL, McKay K, Elmets CA, Kopelovich L, Bickers DR, Athar M. Shh and p50/Bcl3 signaling crosstalk drives pathogenesis of BCCs in Gorlin syndrome. Oncotarget. 2015; 6:36789–36814. [PubMed: 26413810]
13. An KP, Athar M, Tang X, Katiyar SK, Russo J, Beech J, Aszterbaum M, Kopelovich L, Epstein EH Jr, Mukhtar H, Bickers DR. Cyclooxygenase-2 expression in murine and human nonmelanoma skin cancers: implications for therapeutic approaches. Photochem Photobiol. 2002; 76:73–80. [PubMed: 12126310]
14. Chun KS, Akunda JK, Langenbach R. Cyclooxygenase-2 inhibits UVB-induced apoptosis in mouse skin by activating the prostaglandin E2 receptors, EP2 and EP4. Cancer Res. 2007; 67:2015–2021. [PubMed: 17332329]
15. Wiegand, TJ. Nonsteroidal Anti-inflammatory Drug (NSAID) Toxicity. 2016. http://emedicine.medscape.com/article/816117-overview#a4

16. Ray WA, Varas-Lorenzo C, Chung CP, Castellsague J, Murray KT, Stein CM, Daugherty JR, Arbogast PG, Garcia-Rodriguez LA. Cardiovascular risks of nonsteroidal antiinflammatory drugs in patients after hospitalization for serious coronary heart disease. Circ Cardiovasc Qual Outcomes. 2009; 2:155–163. [PubMed: 20031832]
17. Suh N, Reddy BS, DeCastro A, Paul S, Lee HJ, Smolarek AK, So JY, Simi B, Wang CX, Janakiram NB, Steele V, Rao CV. Combination of atorvastatin with sulindac or naproxen profoundly inhibits colonic adenocarcinomas by suppressing the p65/beta-catenin/cyclin D1 signaling pathway in rats. Cancer Prev Res (Phila). 2011; 4:1895–1902. [PubMed: 21764859]
18. Lubet RA, Scheiman JM, Bode A, White J, Minasian L, Juliana MM, Boring DL, Steele VE, Grubbs CJ. Prevention of chemically induced urinary bladder cancers by naproxen: protocols to reduce gastric toxicity in humans do not alter preventive efficacy. Cancer Prev Res (Phila). 2015; 8:296–302. [PubMed: 25762530]
19. Duggan KC, Walters MJ, Musee J, Harp JM, Kiefer JR, Oates JA, Marnett LJ. Molecular basis for cyclooxygenase inhibition by the non-steroidal anti-inflammatory drug naproxen. J Biol Chem. 2010; 285:34950–34959. [PubMed: 20810665]
20. Wang D, Dubois RN. Prostaglandins and cancer. Gut. 2006; 55:115–122. [PubMed: 16118353]
21. Gurpinar E, Grizzle WE, Piazza GA. NSAIDs inhibit tumorigenesis, but how? Clin Cancer Res. 2014; 20:1104–1113. [PubMed: 24311630]
22. Kim MS, Kim JE, Lim DY, Huang Z, Chen H, Langfald A, Lubet RA, Grubbs CJ, Dong Z, Bode AM. Naproxen induces cell-cycle arrest and apoptosis in human urinary bladder cancer cell lines and chemically induced cancers by targeting PI3K. Cancer Prev Res (Phila). 2014; 7:236–245. [PubMed: 24327721]
23. Zelenay S, van der Veen AG, Bottcher JP, Snelgrove KJ, Rogers N, Acton SE, Chakravarty P, Girotti MR, Marais R, Quezada SA, Sahai E, Reis e Sousa C. Cyclooxygenase-Dependent Tumor Growth through Evasion of Immunity. Cell. 2015; 162:1257–1270. [PubMed: 26343581]
24. Xie J, Aszterbaum M, Zhang X, Bonifas JM, Zachary C, Epstein E, McCormick F. A role of PDGFRalpha in basal cell carcinoma proliferation. Proc Natl Acad Sci U S A. 2001; 98:9255–9259. [PubMed: 11481486]
25. Clydesdale GJ, Dandie GW, Muller HK. Ultraviolet light induced injury: immunological and inflammatory effects. Immunol Cell Biol. 2001; 79:547–568. [PubMed: 11903614]
26. Bernard JJ, Cowing-Zitron C, Nakatsuji T, Muehleisen B, Muto J, Borkowski AW, Martinez L, Greidinger EL, Yu BD, Gallo RL. Ultraviolet radiation damages self noncoding RNA and is detected by TLR3. Nat Med. 2012; 18:1286–1290. [PubMed: 22772463]
27. Buckman SY, Gresham A, Hale P, Hruza G, Anast J, Masferrer J, Pentland AP. COX-2 expression is induced by UVB exposure in human skin: implications for the development of skin cancer. Carcinogenesis. 1998; 19:723–729. [PubMed: 9635856]
28. Simon MM, Aragane Y, Schwarz A, Luger TA, Schwarz T. UVB light induces nuclear factor kappa B (NF kappa B) activity independently from chromosomal DNA damage in cell-free cytosolic extracts. J Invest Dermatol. 1994; 102:422–427. [PubMed: 8151120]
29. Gilmore TD. Introduction to NF-kappaB: players, pathways, perspectives. Oncogene. 2006; 25:6680–6684. [PubMed: 17072321]
30. DiDonato JA, Mercurio F, Karin M. NF-kappaB and the link between inflammation and cancer. Immunological reviews. 2012; 246:379–400. [PubMed: 22435567]
31. Li CW, Xia W, Huo L, Lim SO, Wu Y, Hsu JL, Chao CH, Yamaguchi H, Yang NK, Ding Q, Wang Y, Lai YJ, LaBaff AM, Wu TJ, Lin BR, Yang MH, Hortobagyi GN, Hung MC. Epithelial-mesenchymal transition induced by TNF-alpha requires NF-kappaB-mediated transcriptional upregulation of Twist1. Cancer Res. 2012; 72:1290–1300. [PubMed: 22253230]
32. Ricciardi M, Zanotto M, Malpeli G, Bassi G, Perbellini O, Chilosi M, Bifari F, Krampera M. Epithelial-to-mesenchymal transition (EMT) induced by inflammatory priming elicits mesenchymal stromal cell-like immune-modulatory properties in cancer cells. British journal of cancer. 2015; 112:1067–1075. [PubMed: 25668006]
33. Thiery JP, Acloque H, Huang RY, Nieto MA. Epithelial-mesenchymal transitions in development and disease. Cell. 2009; 139:871–890. [PubMed: 19945376]

34. Kalluri R. EMT: when epithelial cells decide to become mesenchymal-like cells. J Clin Invest. 2009; 119:1417–1419. [PubMed: 19487817]

35. Nishitoh H. CHOP is a multifunctional transcription factor in the ER stress response. Journal of biochemistry. 2012; 151:217–219. [PubMed: 22210905]

36. Oyadomari S, Mori M. Roles of CHOP/GADD153 in endoplasmic reticulum stress. Cell death and differentiation. 2004; 11:381–389. [PubMed: 14685163]

37. Tabas I, Ron D. Integrating the mechanisms of apoptosis induced by endoplasmic reticulum stress. Nature cell biology. 2011; 13:184–190. [PubMed: 21364565]

38. Cheng EH, Wei MC, Weiler S, Flavell RA, Mak TW, Lindsten T, Korsmeyer SJ. BCL-2, BCL-X(L) sequester BH3 domain-only molecules preventing BAX- and BAK-mediated mitochondrial apoptosis. Mol Cell. 2001; 8:705–711. [PubMed: 11583631]

39. Tang JY, Aszterbaum M, Athar M, Barsanti F, Cappola C, Estevez N, Hebert J, Hwang J, Khaimskiy Y, Kim A, Lu Y, So PL, Tang X, Kohn MA, McCulloch CE, Kopelovich L, Bickers DR, Epstein EH Jr. Basal cell carcinoma chemoprevention with nonsteroidal anti-inflammatory drugs in genetically predisposed PTCH1+/− humans and mice. Cancer Prev Res (Phila). 2010; 3:25–34. [PubMed: 20051370]

40. Elmets CA, Viner JL, Pentland AP, Cantrell W, Lin HY, Bailey H, Kang S, Linden KG, Heffernan M, Duvic M, Richmond E, Elewski BE, Umar A, Bell W, Gordon GB. Chemoprevention of nonmelanoma skin cancer with celecoxib: a randomized, double-blind, placebo-controlled trial. Journal of the National Cancer Institute. 2010; 102:1835–1844. [PubMed: 21115882]

41. Rundhaug JE, Simper MS, Surh I, Fischer SM. The role of the EP receptors for prostaglandin E2 in skin and skin cancer. Cancer Metastasis Rev. 2011; 30:465–480. [PubMed: 22012553]

42. Lee JL, Kim A, Kopelovich L, Bickers DR, Athar M. Differential expression of E prostanoid receptors in murine and human non-melanoma skin cancer. J Invest Dermatol. 2005; 125:818–825. [PubMed: 16185283]

43. Rundhaug JE, Fischer SM. Cyclo-oxygenase-2 plays a critical role in UV-induced skin carcinogenesis. Photochem Photobiol. 2008; 84:322–329. [PubMed: 18194346]

44. Smith CE, Soti S, Jones TA, Nakagawa A, Xue D, Yin H. Non-steroidal Anti-inflammatory Drugs Are Caspase Inhibitors. Cell Chem Biol. 2017

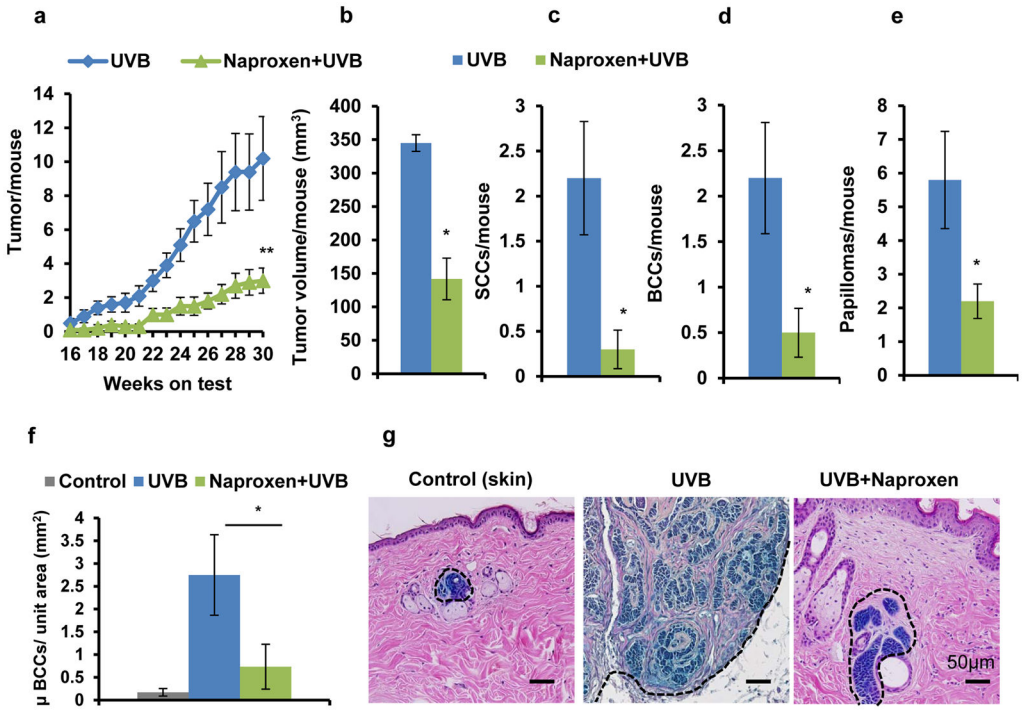

Figure 1. Naproxen inhibits UVB-induced SCC and BCC development in Ptch1$^{+/-}$/SKH-1 hairless mice

(a) tumor/mouse; (b) tumor volume/mouse (mm^3); (c) SCCs/mouse; (d) BCCs/mouse; (e) papilloma/mouse; (f) microscopic BCCs/unit area (mm^2); (g) a representative β-gal staining of microscopic BCCs (blue). * $p<0.05$ and ** $p<0.005$ were considered statistically significant. Animals were administered with naproxen (1 mg/mouse; twice a week) followed by UVB (180 mJ/cm^2) irradiation for 30 weeks. Tumor data were recorded on weekly basis.

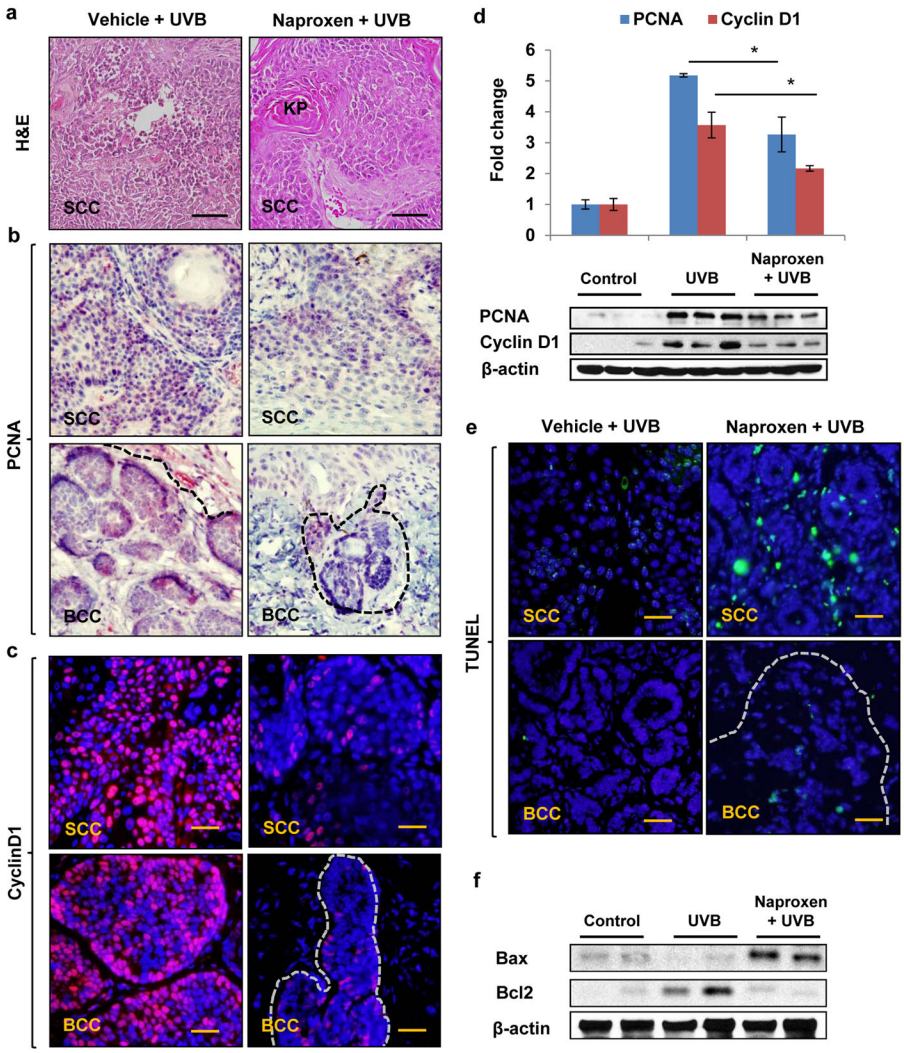

Figure 2. Naproxen reduces proliferation and induces apoptosis in UVB-induced SCC and BCC of Ptch1$^{+/-}$/SKH-1 hairless mice

(a) H&E staining showing histology of SCC; (b) immunohistochemical analysis showing expression of PCNA (red); (c) immunofluorescence staining of cyclin D1 (red); (d) Western blot and densitometric analysis showing epidermal expression of PCNA and cyclin D1; (e) TUNEL-positive apoptotic cells (green); (f) Western blot analysis of apoptosis-related proteins, Bax and Bcl2. Scale bar 20μm. * $p<0.05$ was considered statistically significant.

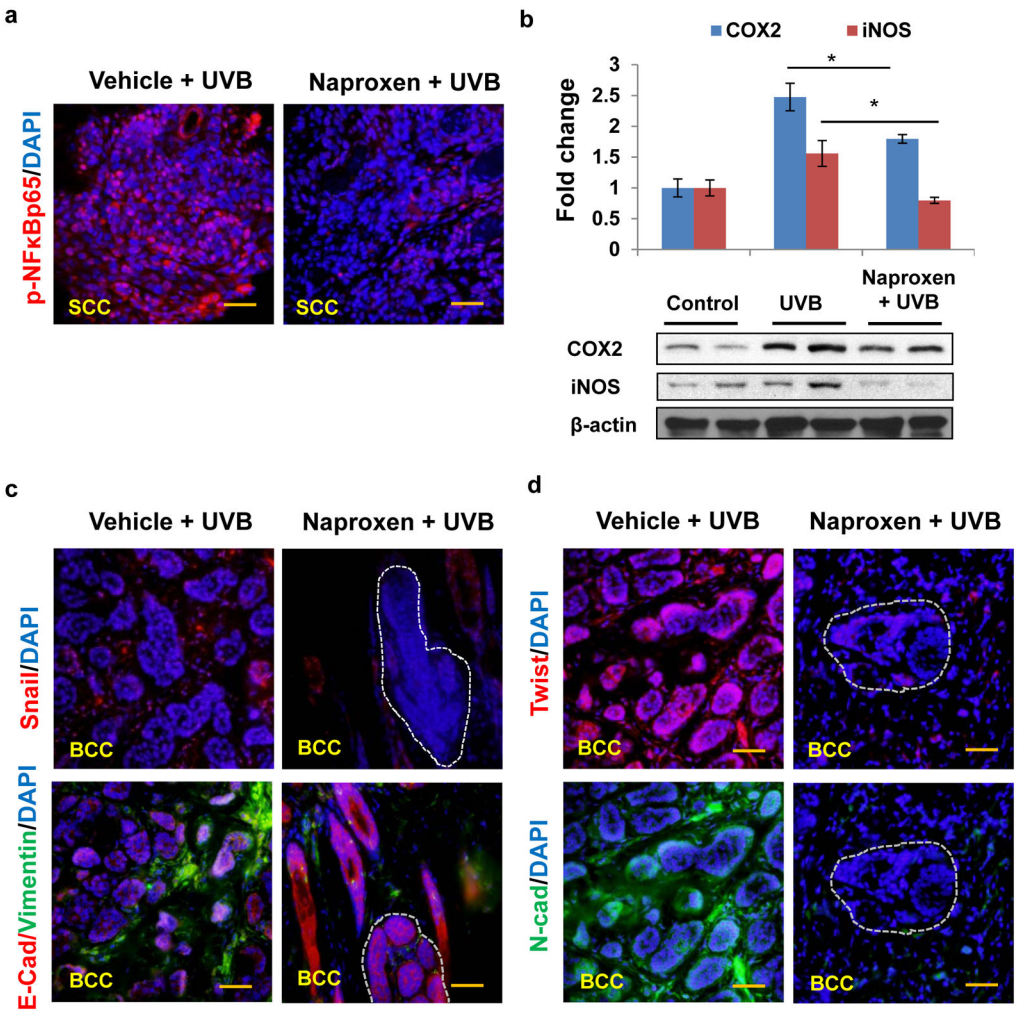

Figure 3. Naproxen diminishes the expression of phosphorylated NFκBp65, pro-inflammatory proteins COX-2/iNOS, and epithelial-mesenchymal transition related proteins

(a) Immunofluorescence staining showing nuclear expression phosphorylated NFκBp65 (red); (b) Western blot and densitometric analysis showing expression of COX-2, and iNOS; (c and d) immunofluorescence staining showing expression of Snail (red), E-cadherin (red), Vimentin (green), Twist (red), N-cadherin (green) (Scale bar 20μm).

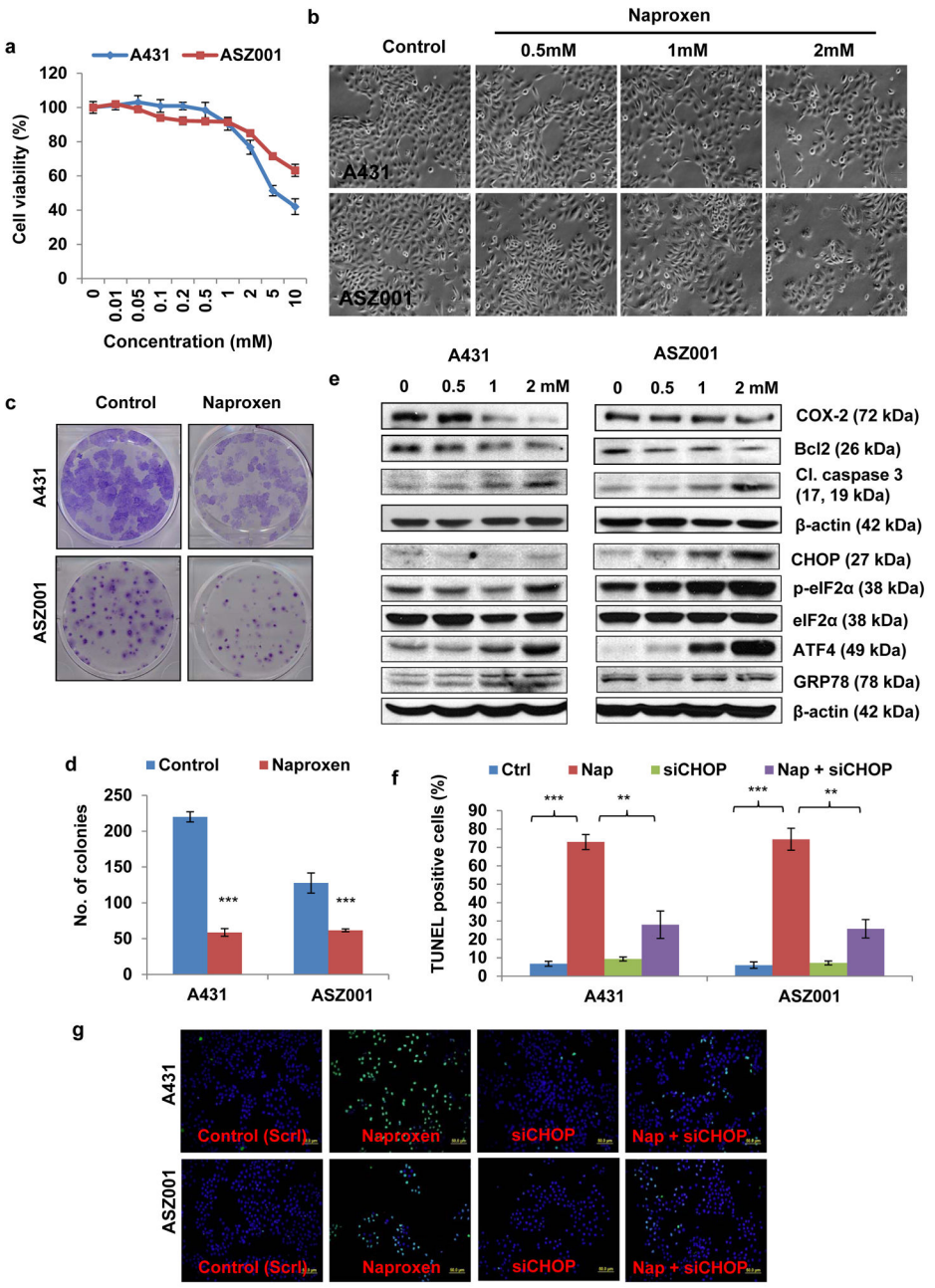

Figure 4. Naproxen activates UPR signaling pathway and induces CHOP-mediated apoptosis in SCC and BCC cells

(a) Cell viability by MTT assay; (b) a representative of A431 and ASZ001 cellular morphology following treatment with naproxen; (c and d) Colony forming assay of A431 and ASZ001 cells treated with naproxen (2 mM); (e) Western blot analysis showing expression of Bcl2, cleaved caspase 3, CHOP, p-eIF2α, eIF2α, ATF4, and GRP78 in A431 and ASZ001 cells treated with naproxen; (f and g) Bar graph showing percentage of TUNEL-positive cells (green). A431 and ASZ001 cells were trypsinized and seeded in 96-well plate. After 24 h, these cells were treated with different concentration of naproxen (0–

10 mM) for 24 h and performed. ** $p<0.005$ and *** $p<0.001$ were considered statistically significant.

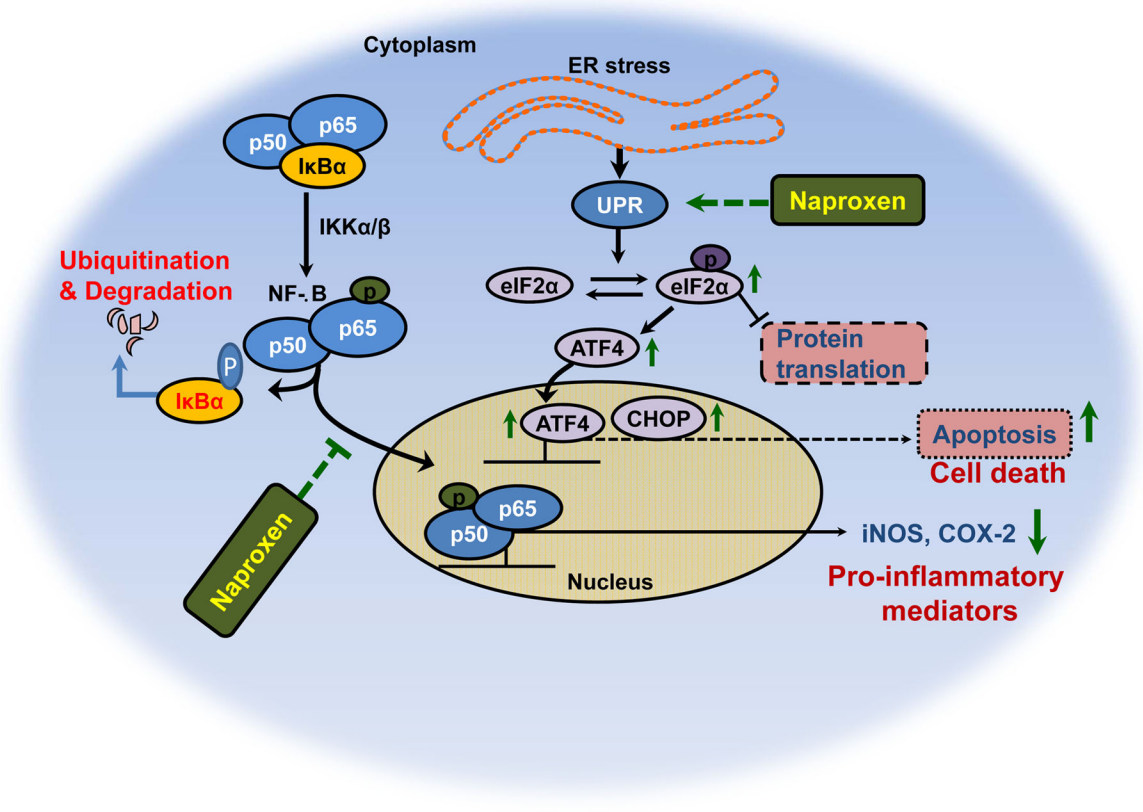

Figure 5. Flow diagram showing potential mechanism of action of naproxen in A431 and ASZ001 cells

Naproxen activates UPR signaling and blocks NFκB pathway. Activation of UPR signaling was characterized by the enhanced phosphorylation of eIF2α and increased ATF4 as well as its transcriptionally regulated CHOP. These pathways together block inflammatory response and induce apoptosis in UVB-induced BCC and SCCs. ↑ represents enhancement, ↓ represents decrease, → represents activating effect, ⊢ represents blocking effect, p – phosphorylation, ER – endoplasmic reticulum, UPR – unfolded protein response, ATF4 - activating transcription factor 4, eIF2α - eukaryotic initiation factor 2α, CHOP - C/EBP homologous protein, NFκB – nuclear factor kappa B, iNOS - inducible nitric oxide synthase, and COX2 – cyclooxygenase2.